

HEAVY QUARK JETS

L.L. Chau, T. Ludlam, F.E. Paige, E.D. Platner, S.D. Protopopescu, P. Rehak
Brookhaven National Laboratory, Upton, New York 11973

I. Motivation

The ability to identify c, b and t jets and to separate them from the much more abundant u, d, s and gluon jets could lead to a wealth of new physics. A very promising technique is the possibility of measuring vertices near the interaction region with a resolution of the order of 10 μ m, making one sensitive to decay lifetimes of a few $\times 10^{-13}$ sec and so tagging charmed particles and possibly τ 's.

The immediate result, of course, would be the measurement of $d^2 \sigma / dp_T dy$ for such jets. This could be compared with QCD predictions, and it would also shine some light on the question of the amount of intrinsic cc, bb and tt in the qq sea of the proton. Detailed study of these jets may allow us to separate t, b and c jets. At sufficiently high p_T (high compared to the t mass) the relative cross sections are expected to be 1/1/1; significant deviations from the expected ratios could lead to the uncovering of new phenomena.

Another interesting possibility is to attempt full reconstruction of B mesons. Given the large background and multiplicities this may seem utopic; however, at $L \sim 10^{32} \text{ cm}^{-2} \text{ sec}^{-1}$, close to 10^{10} B mesons are produced in a year (10^7 sec). This is to be compared with $<10^5$ expected at LEP. So any scheme that selects b jets with $>10^{-4}$ efficiency produces $>10^6$ events for further study. A good example of an interesting decay mode is $B^{\pm} \rightarrow K^{\pm} e^+ e^-$, which is expected from the standard model to have a branching ratio $\sim 10^{-6}$. While such a small branching ratio may be impossible to observe, horizontal gauge symmetry models⁽¹⁾ can raise the branching ratio to $\sim 10^{-4}$, which may be possible at ISABELLE but out of reach at LEP. A branching ratio substantially higher than 10^{-6} cannot be explained in the standard model and would be a very important discovery. Since in this case the decay does not involve charm, one could look for it in the jet accompanying the tagged one; having an identified heavy quark jet will give a tremendous reduction in background. The study of two or more jets will require the capability of doing electromagnetic and hadronic calorimetry over a large solid angle, but the charmed particle tag may be more restrictive in solid angle without a very detrimental effect on efficiency.

Another observation of interest is that of $B^0 \bar{B}^0$ mixing. An initial state of $B^0 (\bar{B}^0)$ can have a finite time-integrated probability of becoming a $\bar{B}^0 (B^0)$. The mixing is maximal when there is equal probability for the final state to be B^0 or \bar{B}^0 irrespective of the initial state (as is the case for $K^0 \bar{K}^0$). There are reasons to believe that, although the mixing for $D^0 \bar{D}^0$ and $T^0 \bar{T}^0$ is small, the mixing for $B^0 \bar{B}^0$ could be maximal.^(2,3) In this case one finds:

$$\sigma(pp \rightarrow B\bar{B}X) = \sigma(pp \rightarrow B\bar{B}X) \sim (1/5 - 1/10) \sigma(pp \rightarrow B\bar{B}X)$$

the factor is 1/10 if only B_d^0 or B_s^0 have maximal mixing and 1/5 if both do. Thus, one can expect that between 20% and 40% of back-to-back b jets end up as $b\bar{b}$ or $\bar{b}b$ rather than $b\bar{b}$. It is sufficient to separate $b\bar{b}$ from $b\bar{b}$ or $\bar{b}b$ jets clearly (at the 10%

level) with 10^{-7} efficiency to observe mixing. The simplest way to accomplish this is to detect equal sign leptons that come from semi-leptonic B decays in back-to-back jets.⁴

ISABELLE will also produce enormous numbers of τ 's ($>10^9$) compared to 10^5 at LEP. For most decays they will be impossible to distinguish from D^{\pm} or F^{\pm} . Nonetheless there are some decay modes worth looking for, such as $\mu^+ e^+ e^-$ or $\mu^+ \phi$. These decays are forbidden in the standard model but could be as large as 10^{-4} with horizontal gauge symmetries, and efficiencies as low as 10^{-4} will be sufficient to reach that level. Finding a signal into such a mode would have momentous impact.

In this exercise we examine the performance of a detector specifically configured to tag heavy quark jets through direct observations of D-meson decays with a high resolution vertex detector. To optimize the performance of such a detector, we assume the small diamond beam crossing configuration as described in the 1978 ISABELLE proposal,⁽²⁾ giving a luminosity of $10^{32} \text{ cm}^{-2} \text{ sec}^{-1}$. The study was carried out with events generated by the ISAJET Monte Carlo⁽³⁾ and a computer simulation of the described detector system.

II. A Heavy Quark Detector

In Fig. 1 we show what a "modest" size heavy quark detector may look like. It needs basically five sections: an inner vertex detector as close to the beam as feasible, a charged particle detector consisting probably of drift chamber planes interleaved with transition radiation detectors to help identify electrons, an electromagnetic calorimeter, a hadronic calorimeter and a μ detector. Because the expected angular spread of jets is large ($> \pm 5^\circ$) we require calorimeters covering $\phi = \pm 45^\circ$ and in rapidity $y = \pm 1$.

The inner vertex detector is shown (actual size) in Fig. 2. It consists of four planes of high resolution position sensing elements. We give a detailed discussion of this device in Sec. IV. To be effective, this detector must be extremely close to the beams. We assume that the first plane is 1 cm from the beam axis. We have discussed this with ISABELLE accelerator physicists and it does not seem to be a fundamental problem provided the chamber is placed either above or below the beams (i.e., not in the horizontal plane). The chamber would be in a rough vacuum separated from the beam by a thin skin ($<250 \mu$ m) of titanium. It would have to be retracted during stacking and acceleration of the beams.

It is natural to imagine repeating the detector arm shown in Fig. 1 four times to achieve full azimuthal coverage, particularly to be able to detect more than one jet. However, for the reason given above, it does not seem feasible to achieve full azimuthal coverage with the vertex detector.

The detector sketched in Fig. 1 will have excellent tracking capability -- the vertex detector alone measures track angles to an accuracy $\lesssim 1$ millirad. It is designed to handle high densities of low momentum tracks. Thus a very modest magnetic field will suffice for adequate momentum measurements. It may

be argued that no magnetic field is necessary, supplanting momentum measurement with calorimetric energy measurement. However, some momentum information will be useful for evaluating multiple scattering errors in the precise vertex measurements; it will be helpful to have measured muon momenta; and information on the signs of tagged leptons may be crucial in some studies. For the present study we have not included the effects of a magnetic field in our calculations.

III. Trigger

The philosophy here is to implement a total energy (E_T) trigger with a calorimeter, and examine the response of the vertex detector for events thus triggered -- i.e., the effectiveness for tagging D meson decays. As we shall see, this effectiveness increases with increasing momentum of the trigger jet. In order to maximize the yield of B mesons, however, we wish to keep the E_T threshold as low as possible.

With the calorimetric trigger alone the major background is due to light quark jets. Therefore we consider a "low" E_T trigger (15 GeV in the calorimeter) with lepton triggers in coincidence. Since the leptons of interest are relatively soft, triggers on leptons are not straightforward, and will require some real-time processing. The choice of 15 GeV E_T threshold is guided by our estimates of lepton trigger capability, for the luminosity of 10^{32} cm⁻² sec⁻¹. We also consider a "high" E_T threshold of 30 GeV, and a "low-low" threshold of 8 GeV.

Calorimeter Trigger

The hadron calorimeter is 1.5 meters from the interaction diamond and is 3x3 m² in area. Fine segmentation is important. It is subdivided into 20x20 cm² towers ($\sqrt{250}$ cells). The electromagnetic shower detector (approximately the first 10 radiation lengths of the calorimeter) is subdivided into 1000 cells. The full calorimeter is 6 absorption lengths deep.

Since we are triggering at relatively low E_T , the energy resolution of the calorimeter is a critical determinant of trigger rates. A calorimeter with hadronic energy resolution $\sigma_E = .8\sqrt{E}$ (typical of iron/scintillator devices) would give a trigger rate several times the rate at $E_T = 15$ GeV. Using the "best" hadron calorimeter, with $\sigma_E \approx .3\sqrt{E}$ (e.g. uranium/scintillator), the trigger rate will be 30-50% higher than the true rate. For the results presented here we do not include the effect of calorimeter resolution on the rates.

At $L = 10^{32}$ cm⁻² sec⁻¹ we have 6×10^6 interactions/sec, most of which send something into the calorimeter. Hence the mean time between events is $\sqrt{200}$ nsec for a calorimeter trigger. For reasonable calorimeter gate widths ($\sqrt{100}$ nsec) this results in a substantial contribution to the trigger rate due to pile-up. If, however, we require that each cell of the calorimeter have a minimum energy before adding it to the trigger sum (250 MeV for the EM part, 500 MeV for the hadronic part) the rate due to pile-up of "minimum bias" events is suppressed well below the jet trigger rate for $E_T \gtrsim 5$ GeV.

The calorimeter trigger rates for our 3 chosen E_T thresholds are given in the first line of Table I. The corresponding rates for b-quark jets among these triggers is given on the second line. It will be seen that the ratios of triggers/b-quark jets are $\sqrt{1000}$, 400, 300 for E_T thresholds of 8 GeV, 15 GeV, 30 GeV, respectively. For the 15 GeV threshold we

have $\sqrt{1}$ b-jet/sec among the triggers, and we need to bring the trigger rate down by another factor of 10-20 to reach a reasonable rate for data recording.

Fig. 3 shows the multiplicity of charged tracks into the detector for minimum bias events and for a trigger threshold of 15 GeV. These include only tracks which traverse all four planes of the vertex detector. Because of the small diamond size the fraction of tracks which do otherwise is small: For $E_T > 15$ GeV the mean number of hits in the first plane of the vertex detector is 9.8.

In Fig. 4 we show the momentum spectra of charged tracks in the detector for the 15 GeV threshold setting. Note that the leptons shown in 4b and 4c come from both B meson and D meson decay. (Fig. 4b also includes Dalitz electrons.)

Muon Trigger

For the detector configuration shown in Fig. 1, with a 6 absorption length calorimeter, the energy loss suffered by a muon is 1.5 GeV. Thus a trigger on muons traversing the calorimeter is limited to $P_\mu \gtrsim 2$ GeV/c, or about 70% of the muons from B and D meson decay (see Fig. 4).

The probability for a pion to traverse the calorimeter without interacting (punch-through) and thus fake a muon is .0025. The probability for a pion (kaon) to produce a decay muon before absorption in the calorimeter is $.029/P_\pi$ ($.22/P_K$). We take a K/ π ratio .2, and assume that only particles with $P > 2$ GeV/c will produce a fake muon trigger by punch-through or decay.

For calorimeter-triggered events, the mean number of charged particles entering the calorimeter is $\sqrt{9}$ (see Fig. 3), of which 18% have $P > 2$ GeV/c for a calorimeter threshold of 30 GeV.

Given these numbers we can construct the following table of minimum background rates for a muon trigger in coincidence with the calorimeter trigger (at luminosity = 10^{32} cm⁻² sec⁻¹):

E_T Threshold	Punch-Through	π, K Decay Muons
8 GeV	10 sec ⁻¹	62 sec ⁻¹
15	1.5	9
30	.05	.5

Thus the trigger rate can, in principle, be reduced by a factor of 30-40 from that given by the calorimeter alone (Table I). To achieve this, however, we must deal with additional severe background due to leakage of shower particles out the back of the calorimeter. This can be reduced to levels comparable to those in the table above by the following two means, both of which require a fast processor if they are to be implemented at the trigger level:

- i) Require a minimum ionizing signal in the calorimeter segments traversed by the "muon."
- ii) Require that the position and angle of the track exiting the calorimeter match, within multiple scattering limits, the trajectory of a charged particle incident on the calorimeter.

For lack of a detailed study (but guided by a similar study done by the R807 Group) we take the muon trigger rate to be roughly twice the "minimum" rate due to punch through and decay. This crude estimate of rates is entered in Table I for calorimeter plus muon trigger. Note that the addition of a muon trigger is useless for $E_T > 30$ GeV (for this detector configuration) and in fact the signal-to-background ratio is not greatly improved by the muon trigger for any of the three E_T threshold settings.

Electron Trigger

For the e-trigger we choose transition radiation detectors (TRD) because of the high degree of segmentation required and the desire to separate electrons from hadrons over a wide range of energies with a compact device.

We assume a total length of ~ 80 cm of TRD, subdivided into two separate modules as shown in Fig. 2. Each module is made up of ~ 5 planes of radiator (Li foils or Carbon Fibers), each with MWPC readout. Such a device should be capable of reducing the π/e rate by a factor of $\sim 10^3$, with good efficiency for electrons of momenta $\gtrsim 1$ GeV/c. (We are specifically guided by the configuration tested in Ref. 4). Such a device, coupled with the EM calorimeter will give a very powerful electron tag. At the trigger level, however, the counting rate will be dominated by conversion electrons, as the TRD thickness will be $\sim 5\%$ of a radiation length.

We estimate that $\sim 1/20$ of the calorimeter triggered events will have a conversion electron with $p > 1$ GeV/c. This background can be virtually eliminated by requiring that the electron track appear in all four planes of the vertex detector, but it is unlikely that this can be accomplished at the trigger level. Some improvement can certainly be had with an on-line processor, e.g., by requiring the electron track to appear in the first of the two TRD modules. Guided by these considerations, the entries in Table I are based on the assumption that the electron trigger reduces the calorimeter trigger rate by a factor of 30, and is 90% efficient for electrons.

IV. Vertex Detector

The use of semiconductor detectors as very high resolution tracking devices in high energy physics experiments has been a subject of intense development over the past few years.⁽⁵⁾ A number of such detectors are being constructed (one is operational)⁽⁶⁾ which give ~ 10 μm space-point resolution in the high track density environment of heavy quark searches at fixed target machines. These "microstrip" detectors consist of silicon wafers whose surface area is finely subdivided into strips; each strip may be read out as a separate detection element. The strip-to-strip spacing is typically 20-50 μm . This gives the characteristic position resolution, which is achieved along one coordinate of the detector.

The signal charge for a minimum ionizing track is $\sim 8 \times 10^4$ electron-hole pairs per mm of detector thickness, with charge collection time $\lesssim 50$ nsec for a 300 μm thick detector. This, coupled with the intrinsically high degree of segmentation, leads to excellent rate capability. The lifetime of such detectors has been measured to exceed $10^{14}/\text{cm}^2$ for fluxes of relativistic charged particles. For the detector geometry discussed here, the innermost plane of the vertex detector would see an integrated flux of $\sim 2 \times 10^{12}$ charged particles/ cm^2 in a year of running at a luminosity of $10^{32} \text{ cm}^{-2} \text{ sec}^{-1}$. The effects of

background radiation need more study: slow neutrons and heavily ionizing particles are much more damaging than minimum ionizing particles. Tests carried out with silicon surface-barrier detectors placed near the beam crossing at the ISR indicate that these backgrounds will not be a problem, however.

The most serious technical difficulty for implementing these detectors in colliding beams is the extremely high density of output connections in a situation where we need to cover (relatively) large area. An output on each strip implies thousands of connections per centimeter along the detector edge. One way out, which is being studied at BNL, is to use resistive charge division to interpolate the position among groups of strips. An analysis by V. Radeka⁽⁷⁾ gives the following formula for the optimal number of outputs as a function of detector characteristics:

$$N = \xi_a^{2/3} \frac{A}{t(\sigma_x w)^{2/3}} \quad \text{IV.1}$$

where

- σ_x = resolution
- A = detector area
- t = detector thickness
- w = strip length
- $\xi_a^{2/3} = 1.4 \times 10^{-2} \text{ cm}^{1/3}$ for silicon detectors
- N = number of signal outputs.

For $\sigma_x = 10$ μm and $t = 300$ μm (a standard wafer thickness for semiconductor devices) one obtains

$$N = 47 \frac{A}{w^{2/3}} \quad \text{IV.2}$$

For the detector illustrated in Fig. 2 this gives, for the four planes,

$$170 + 317 + 462 + 640 \approx 1600$$

total readout channels.

Note that our detector measures one coordinate only. We take this to be the azimuthal coordinate. To obtain space points in 2 dimensions (using strip detectors) would require at least 3 times as many detector planes. As we shall see, the cost in multiple scattering errors would outweigh the usefulness of such a scheme. Thus the proposed detector really provides a tag for charmed particles and not a fully reconstructed vertex.

It should be pointed out that other schemes for realizing semiconductor devices as track detectors of this type are being considered and developed by various groups. For instance, CCD devices could, in principle, solve both the "connection" and the 2-dimensional readout problems; however, these (as track detectors) are in a very early stage of development and are fundamentally unsuited for the rates encountered in ISABELLE experiments. A device with strip electrode geometry but serial readout (hence few connections) is being developed at the University

of Pittsburgh.⁽⁸⁾ This is based on a very interesting technique in which signal charge is stored in shallow impurity traps in the i-region of a PIN diode detector at cryogenic temperatures. These and other developments may point the way to better devices than that proposed here. For the moment, we confine our analysis to the "known" technology of microstrip detectors.

For a 4-plane detector, the error (σ_v) in the extrapolation of a track to the vertex position is given by (see Fig. 5):

$$\sigma_v^2 \approx \frac{\sigma_x^2}{4} + \left(\frac{\sigma_x}{\sqrt{3}} \frac{L_1}{L_2} \right)^2 + \left(\frac{8.7 \times 10^{-4}}{\beta P \text{ (GeV)}} L_1 \right)^2.$$

The first term is the position resolution, the second is the effect of the angular resolution and the last is the multiple scattering contribution. For $\sigma_x = 10 \mu\text{m}$, $L_1 = 1 \text{ cm}$, $L_2 = 2 \text{ cm}$:

$$\sigma_v^2 \approx (5 \mu\text{m})^2 + (3 \mu\text{m})^2 + \left(\frac{9}{\beta P} \mu\text{m} \right)^2.$$

Multiple scattering dominates for $P \gtrsim 2 \text{ GeV}/c$ even though we have been at some pains to place the detector as close to the beams as feasible ($L_1 = 1 \text{ cm}$). Nonetheless, for the average momenta of tracks through the detector in E_T -triggered events (Fig. 4) we obtain $\sigma_v \approx 10 \mu\text{m}$.

The average multiplicity of charged tracks into our detector, for calorimeter triggered events, is $\sqrt{9}$ (Fig. 3), and the distribution ranges up to about 20. From these tracks we must reconstruct the primary vertex and determine which, if any, tracks originate from a secondary decay vertex. For our Monte Carlo simulations we conservatively included only D^\pm decays and used a lifetime for them of $8 \times 10^{-13} \text{ sec}$. The distribution of projected miss distance, δ , is shown in Fig. 6. The criteria for resolved decays were as follows: (Note that σ_v is momentum-dependent.)

- i) If only a single decay track is visible, it must have

$$\delta > \max(100 \mu\text{m}, 4 \sigma_v)$$
- ii) If two decay tracks are visible,

$$\delta > \max(50 \mu\text{m}, 4 \sigma_v)$$
- iii) If more than two decay tracks are visible,

$$\delta > \max(50 \mu\text{m}, 3 \sigma_v)$$
- iv) If a decay lepton is tagged,

$$\sigma > \max(50 \mu\text{m}, 3 \sigma_v)$$

for all visible track multiplicities.

The results are shown in Table II for various decay topologies and E_T thresholds. Roughly 40% of the charged D mesons entering the vertex detector are resolved. This means that $\sqrt{20}\%$ of the triggered heavy quark jets have a visible decay. The rates for accumulating events with resolved decays are shown in Table I.

Cut (i) is the least restrictive; a 4σ cut keeps only $\sqrt{1/16000}$ tracks. However, since the average number of tracks per event is 10, the probability of a fake decay is $\sqrt{1}$ per 1600 events. Since the cuts reduce the signal by a factor of 6 (a factor of 2 by requiring D^\pm and another factor of 3 from lifetime cut) the overall improvement in signal-to-background ratio (S/B) is $\sqrt{200}$. From Table I we can see that once a lepton trigger is used the vertex detector cuts increase S/B to 1/1. Off-line the lepton identification can be substantially improved, particularly for electrons by correlating TRD and shower counter information. Therefore, it is possible to reduce the light quark jet background to the 10%-20% level. The only significant background to b jets at this point is from c jets.

V. Physics with Two Detectors

Two detectors, like the one shown in Fig. 1, placed opposite each other, offer very interesting physics possibilities. In Table III we give the rates for various triggers using both detectors. The triggers require a minimum total energy (E_T) deposition in the calorimeter and in triggers, 3, 4, 5 there is also an electron with $P_e > 1.0 \text{ GeV}/c$ (two in trigger 5).

Consider, for example, trigger 4, which has a comfortable trigger rate (8 sec^{-1}). After a vertex cut on the jets in the detector with an electron trigger the signal-to-background ratio S/B is 1/1. This can be reduced by at least another factor of 5 to 10 by additional off-line requirements on the electron, such as matching momentum measured in the drift chambers with energy deposition in the electromagnetic calorimeter. This gives an unbiased sample of b jets in the opposite detector with a background of c jets only (roughly 2 to 1). In 10^7 sec we have then 2×10^5 heavy quark jets of which 7×10^4 are b jets. This is to be compared with $\sqrt{10^5}$ b jets that are produced at LEP in a similar period of time before any selections are made.

It may be possible to reduce the data rate by a factor of $\sqrt{10}$ by using information on the multiplicity and pattern of space points in the vertex detector at the trigger level. If so, then triggers 2 and 3 can ultimately provide as many as 10^6 tagged b jets.

Trigger 5, which requires 2 electrons in one detector, is not very efficient for b jets, but it is of great interest for searching for rare decays, such as $B^\pm \rightarrow K^\pm e^+ e^-$ or $\tau^\pm \rightarrow \mu^\pm e^+ e^-$. If all B^\pm decayed to $K^\pm e^+ e^-$ we would have 2.2 events/sec (trigger 1). Requiring $P_e > 1.0 \text{ GeV}/c$ and $P_K > 1.5 \text{ GeV}/c$ reduces the rate to 0.20 sec^{-1} so after a vertex cut on the detector opposite to the one triggering on 2 electrons we would collect $\sqrt{3} \times 10^5$ Kee decays in 10^7 sec . The only significant background at this level are the few percent of b jets which produce 2 electrons. After requiring $P_K > 1.5 \text{ GeV}/c$ (no K identification), $P_e > 1.0 \text{ GeV}/c$ and $m(\text{Kee}) = m(B) \pm 50 \text{ MeV}$ the b jet background is down to $\sqrt{1/40,000}$. Thus a branching ratio for $B^\pm \rightarrow K^\pm e^+ e^- > 10^{-5}$ could be observed. A slightly higher branching ratio could be seen for $\tau \rightarrow \mu e e$ (using τ 's from B and F decays).

In the search for $B\bar{B}$ mixing we can use trigger 3 with the additional requirements of observing a lepton in both arms. Because of the chain decays $b \rightarrow c \rightarrow l$ and $b \rightarrow c \bar{c} s$ with $c \rightarrow l$ the leptons observed could be of equal sign even in the absence of mixing. However, the leptons that come from $b \rightarrow l$ have substantially higher momentum than the secondary leptons, as

shown in Fig. 7. We make the requirements that both leptons have $P_e > 4.0$ GeV/c, that a D be tagged in each arm, and finally that the leptons be within 30μ from the primary vertex (to reduce the number of leptons from D decay). Then the equal sign pair are reduced to less than 10% of the direct pairs.

With the above cuts one expects $\sqrt{35,000}$ pairs from direct BB leptonic decay and less than 3,000 where one lepton comes from the decay chain $B \rightarrow c \rightarrow \ell$ (in 10^7 sec at $L=10^{32}$ cm^{-2} sec^{-1}). Unequal sign leptons can also come from cc pair; however, the simultaneous requirements that a D be tagged and that the lepton be within 30μ of the primary vertex reduce the expected number to $\sqrt{6,000}$. This number can be reduced further by studying the P_T distribution of the leptons with respect to the jet axis, so they are not a significant background. A possible source of background of equal sign leptons is due to cc or cc jets. For $|y| < 1$ these are expected to have a much smaller cross section than the bb jets and thus negligible.

Given the large number of lepton pairs from direct B decays ($\sqrt{35,000}$) satisfying the selection criteria described above and the relatively low background, detailed studies of the characteristics of these events are possible and should enable one to show convincingly the existence or non-existence of BB oscillations.

Conclusion

We have shown that it is possible in principle to design a detector of modest dimensions capable of detecting heavy quark jets with good rejection of light quark (and gluon) jets. In order to achieve this, good lepton identification and the ability to tag a charmed particle decay with a high resolution vertex detector are indispensable. To keep the vertex detector within realistic dimensions we make use of the possibility at ISABELLE of a small interaction diamond (± 2 cm full width) with high luminosity, $L=10^{32}$ cm^{-2} sec^{-1} .

With two detectors placed opposite to each other it is possible to collect at least 2×10^5 unbiased heavy quark jets (in the detector opposite the tagged jet) in a year of running with practically no background from other processes. More sophisticated on-line data processing could raise this number to 2×10^6 . The ratio of c to b jets in this sample is 2 to 1. With such large numbers of B mesons it is conceivable that some decay modes may be fully reconstructed. Of particular interest is the decay $B^\pm \rightarrow K^\pm e^+ e^-$ for which an upper limit of 10^{-5} is achievable, easily an order of magnitude better than what is possible at LEP. The standard model predicts 10^{-6} for this branching ratio; however, horizontal gauge symmetries can increase it to 10^{-4} which would be observable with the detectors envisaged here.

This research was supported by the U.S. Department of Energy under contract DE-AC02-76CH00016.

Table I

Rates with One Detector at $L = 10^{32}$ cm^{-2} sec^{-1}

	$E_T > 8$ (sec^{-1})	$E_T > 15$ (sec^{-1})	$E_T > 30$ (sec^{-1})
<u>Calorimeter Only:</u>			
Trigger rate	7000.	560.	12.
B Jets	6.0	1.4	.04
B \rightarrow Resolved D^\pm	1.0	.24	.008
<u>Calorimeter + Muon</u>			
<u>Trigger:</u>			
Trigger rate	350.	40.	2.
B Jets	.7	.16	.004
B \rightarrow Resolved D^\pm	.1	.03	.0012
<u>Calorimeter + e Trigger</u>			
Trigger rate	250.	20.	.4
B Jets	1.0	.24	.007
B \rightarrow Resolved D^\pm	.16	.04	.0014

Table II

	Resolved D^\pm		
	Total D^\pm in Trigger Jet	vs.	E_T Threshold
	$E_T > 8$	$E_T > 15$	$E_T > 30$
1 Visible Track	20%	24%	25%
2 Visible Tracks	11	9	8
>2 Visible Tracks	7	8	14
Total	38%	41%	47%
Visible Lepton	12%	12%	13%

Table III

Rates with Two Detectors at $L = 10^{32}$ sec^{-1} cm^{-2}

	Trigger Configuration		Trigger Rate sec^{-1}	b jet Rate*
	Detector 1	Detector 2		
1	$E_T > 8$	$E_T > 8$	2200	2.2
2	$E_T > 15$	$E_T > 15$	130	0.24
3	$e+E_T > 8$	$E_T > 8$	120	0.40
	$E_T > 8$	$e+E_T > 8$		
4	$e+E_T > 15$	$E_T > 15$	8	0.04
	$E_T > 15$	$e+E_T > 15$		
5	$2e+E_T > 8$	$E_T > 8$	4	0.005
	$E_T > 8$	$2e+E_T > 8$		

*The b jet rate is for b jets in the detector that requires no electron in the trigger.

References

1. D.R.T. Jones, G.L. Kane, J.P. Leveille, Nucl. Phys. B198, 45 (1982).
2. J. Sanford et al., BNL 50718 (January 1978).
3. Frank E. Paige and S.D. Protopopescu, BNL-29777. This study was done using the latest version, ISAJET 3.24.
4. C. Fabjan et al., Nucl. Instr. Meth. 185, 119 (1981).
5. For the proceedings of a recent workshop on the subject, see "Silicon Detectors for High Energy Physics," T. Ferbel, Ed. (Fermilab, 1982).
6. B. Hyams et al., CERN Exp. NA-14 (see Ref. 2, p. 195).
7. V. Radeka and R. Boie, IEEE Trans. Nucl. Sci., NS (1979); see also Ref. 2, p. 21.
8. P. Shephard et al., Ref. 2, p. 73.

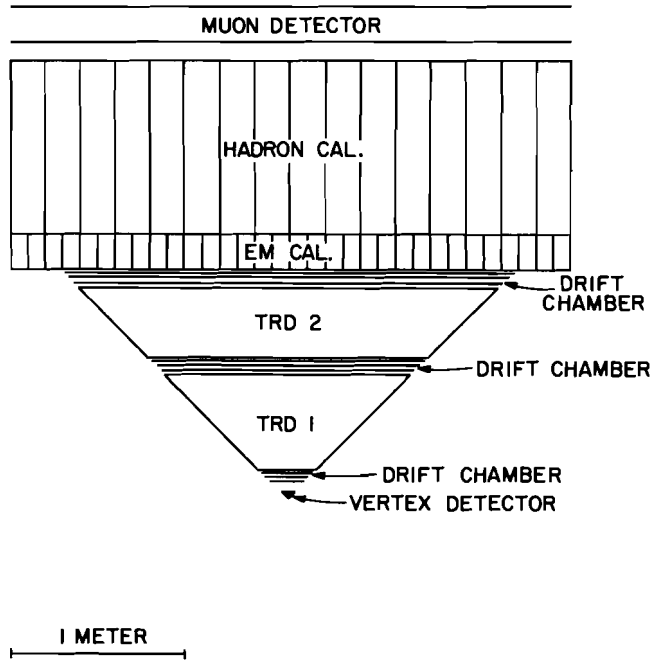


Figure 1. Single arm heavy quark detector at $\theta = 90^\circ$, covering ± 1 units of rapidity and 45° in azimuth.

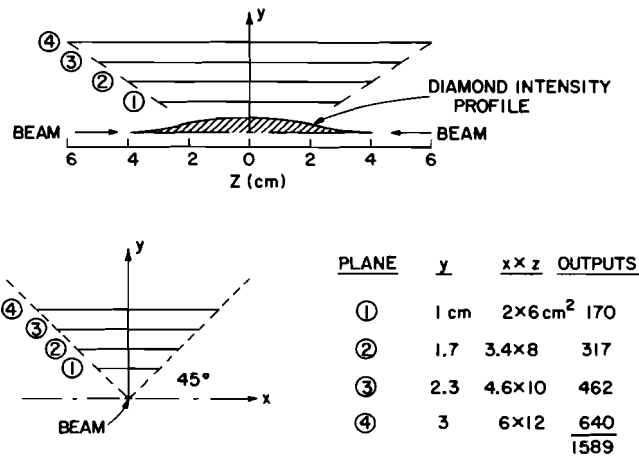


Figure 2. Four plane vertex detector, shown full size.

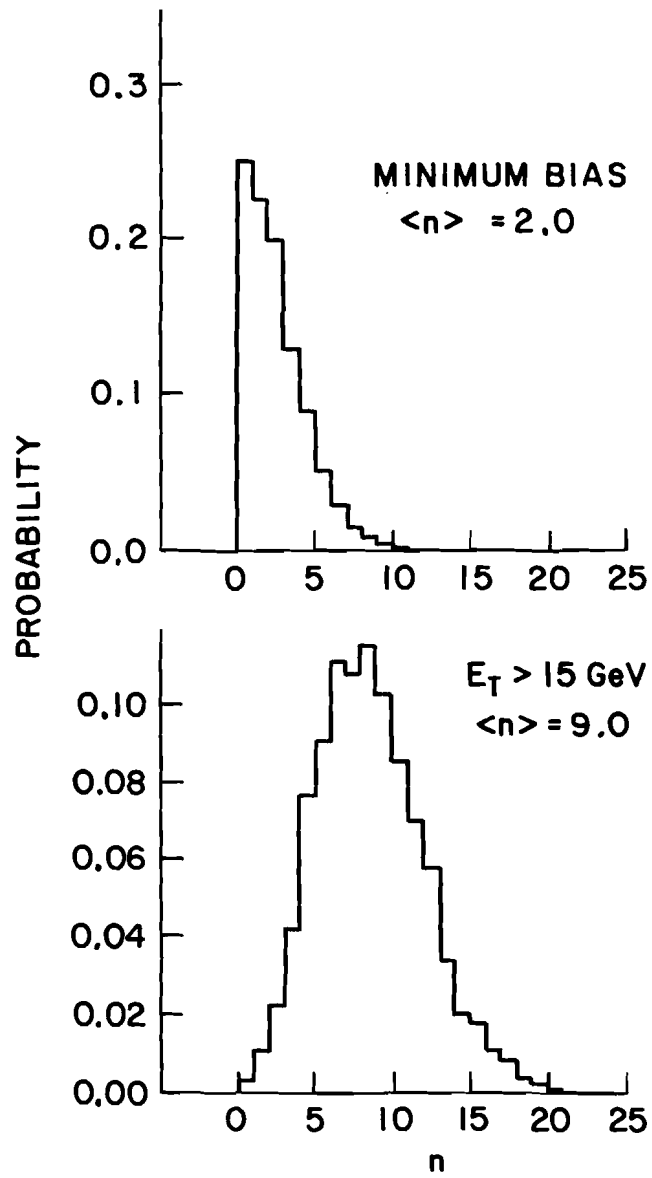


Figure 3. Multiplicity of charged tracks through the detector.

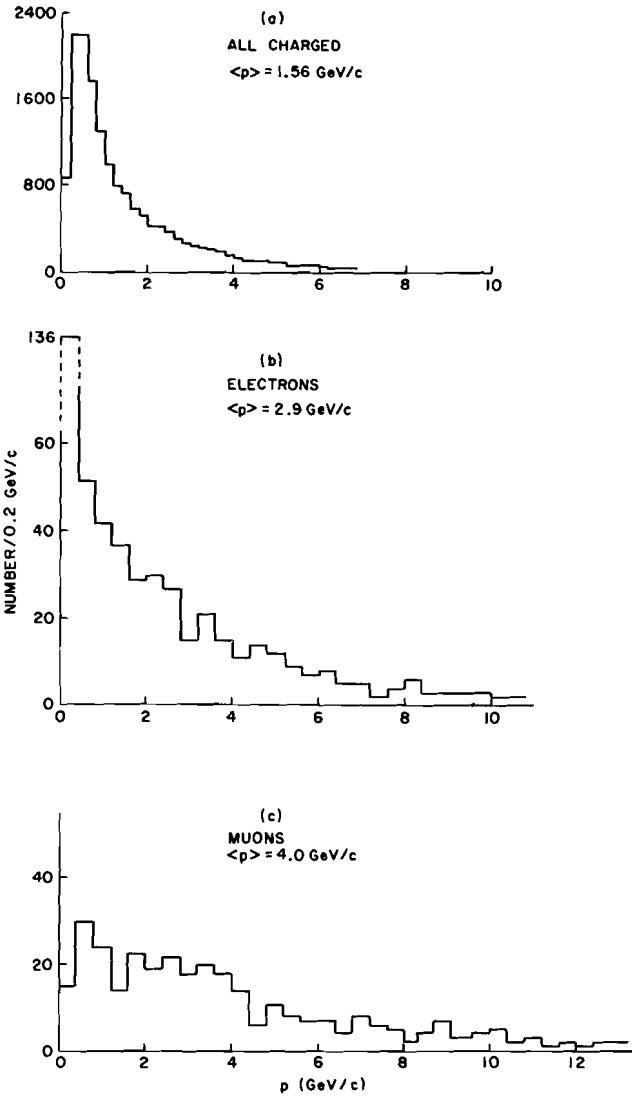


Figure 4. Momenta of charged tracks in the detector for trigger threshold $E_T > 15 \text{ GeV}$.

- (a) All charged tracks
- (b) Electrons (including Dalitz decay of π^0, η)
- (c) Muons

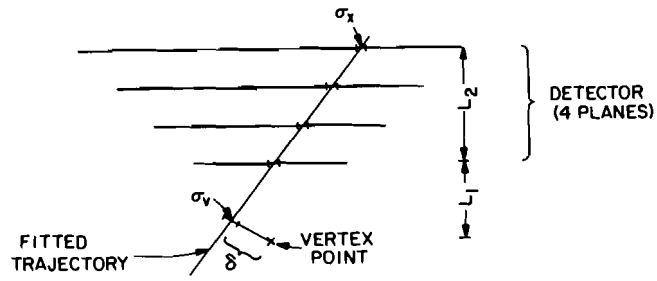


Figure 5. Resolution at the vertex for a single track (not to scale).

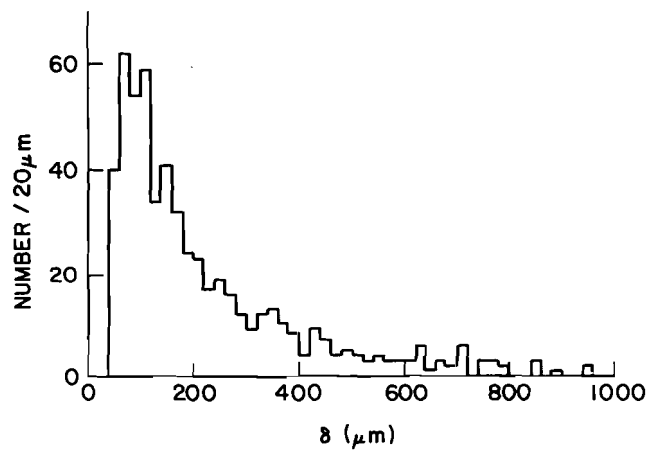


Figure 6. Projected miss distance for resolved decay tracks of D^\pm mesons, using the criteria given in the text.

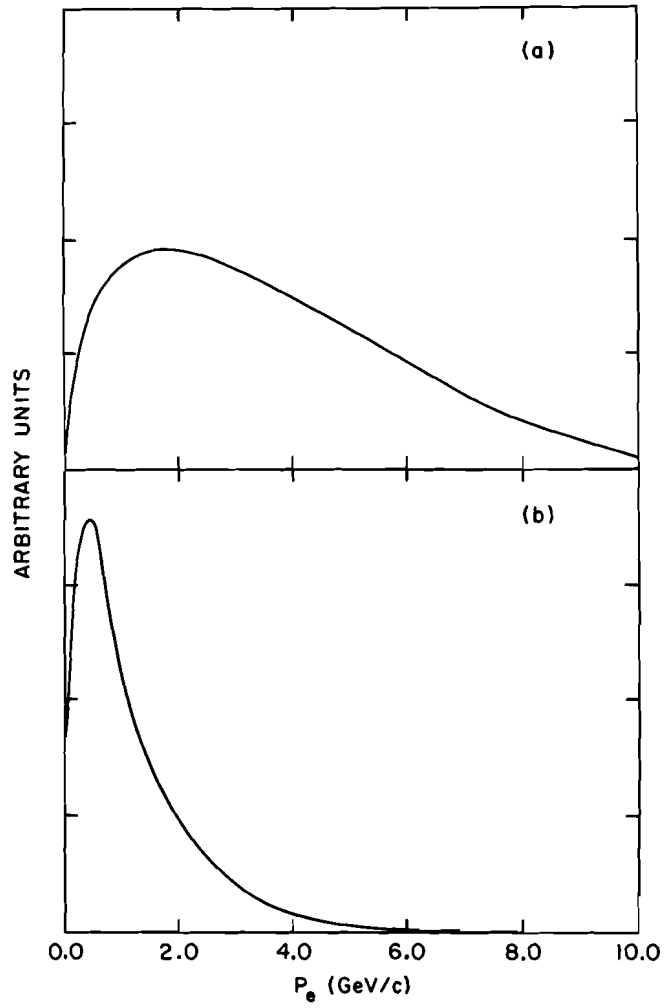


Figure 7. (a) Momentum distribution of leptons from semi-leptonic B decays.

(b) Momentum distribution of leptons from the chain decay $b \rightarrow c \rightarrow \ell$.